

# Excitation of the $\Delta$ (1232)-resonance in proton-nucleus collisions $\star$

M. Trzaska<sup>1</sup>, D. Pelte<sup>1</sup>, M.-C. Lemaire<sup>2,3</sup>, J.P. Alard<sup>4</sup>, J. Augerat<sup>4</sup>, D. Bachelier<sup>5</sup>, N. Bastid<sup>5</sup>, J.-L. Boyard<sup>5</sup>, C. Cavata<sup>2</sup>, P. Charmensat<sup>4</sup>, J. Cugnon<sup>7</sup>, P. Dupieux<sup>4</sup>, P. Gorodetzky<sup>6</sup>, J. Gosset<sup>2</sup>, T. Hennino<sup>5</sup>, J.-C. Jourdain<sup>5</sup>, A. LeMerdy<sup>2</sup>, D. L'Hôte<sup>2</sup>, B. Lucas<sup>2</sup>, J. Marroncle<sup>4</sup>, G. Montarou<sup>4</sup>, M.-J. Parizet<sup>4</sup>, J. Poitou<sup>2</sup>, D. Quassoud<sup>4</sup>, P. Radvanyi<sup>3</sup>, B. Ramstein<sup>5</sup>, A. Rahmani<sup>4</sup>, M. Roy-Stephan<sup>5</sup>, O. Valette<sup>2</sup>, J. Vandermeulen<sup>7</sup>, and P. Zupranski<sup>3</sup>

<sup>1</sup> Physikalisches Institut, Universität Heidelberg, Philosophenweg 12, W-6900 Heidelberg, Federal Republic of Germany

<sup>2</sup> DPhN, CEN Saclay, F-91191 Gif-sur-Yvette Cedex, France

<sup>3</sup> LNS, CEN Saclay, F-91191 Gif-sur-Yvette Cedex, France

<sup>4</sup> LPC, Clermont-Ferrand, F-63177 Aubière Cedex, France

<sup>5</sup> IPN, Orsay, BP N°1, F-91406 Orsay, France

<sup>6</sup> CRN, BP 20 CR, F-67037 Strasbourg Cedex, France

<sup>7</sup> Liège University, B-4000 Sart Tilman, Belgium

Received April 10, 1991

The excitation of the  $\Delta$  resonance is observed in proton collisions on C, Nb and Pb targets at 0.8 and 1.6 GeV incident energies. The mass  $E_0$  and width  $\Gamma$  of the resonance are determined from the invariant mass spectra of correlated  $(p, \pi^\pm)$ -pairs in the final state of the collision: The mass  $E_0$  is smaller than that of the free resonance, however by comparing to intra-nuclear cascade calculations, this reduction is traced back to the effects of Fermi motion, NN scattering and pion reabsorption in nuclear matter.

**PACS:** 25.40.Vc; 14.20.Gt

## 1. Introduction

The study of intermediate-energy nucleus-nucleus collisions is of great interest, because it is the only way to lift, under laboratory conditions, nuclear matter from its ground state into the state of high density and temperature. Some years ago, pion production was proposed to be a particular sensitive probe for the equation of state of nuclear matter [1]. Since then, several theoretical studies of nucleus-nucleus collisions in the framework of BUU and QMD calculations, which included momentum dependent forces [2] or modified the properties of baryons in nuclear matter [3], have suggested, that pion production is probably not such a clear and unambiguous probe for the nuclear EOS as anticipated. To clarify the situation, a better understanding of pion-production in nucleus-nucleus and proton-nucleus collisions is needed.

For this purpose, charged pion multiplicities have been measured in non-inclusive proton-nucleus interactions at 0.8 and 1.6 GeV [8]. The comparison of experimental mean values and dispersions to predictions given

by intra-nuclear-cascade calculations [10, 11] displays discrepancies even for such an elementary probe. Since in NN interactions the pion production is known to originate predominantly from  $\Delta$ -decay, it was interesting to study the  $\Delta$ -excitation in the same data.

The identification of this  $\Delta$ -excitation in nucleus-nucleus collisions is rather difficult because of the high particle multiplicity in the final state the collision [4, 9]. Therefore, energy-loss measurements in the entrance-channel of the charge-exchange  $A(^3\text{He}, t)$  reaction were formerly used to investigate the mechanism of  $\Delta$ -excitation in nuclear matter [5]. In these experiments a shift in the effective  $\Delta$ -mass was found, when massive targets are compared with charge-exchange on protons. Part of this shift can be explained by trivial effects like form factors, Pauli blocking and Fermi motion, but a significant rest remains, which was attributed to a coherent propagation of pions in the nuclear medium [6].

A direct observation of  $\Delta$ 's in nuclei by detecting their decay particles proton and pion in the final state of the collision were first achieved with proton-induced nuclear reactions in [12]. In this experiment a quasi-free nature of the process was ensured by demanding a fast proton being emitted under forward angles. This requirement effectively selects peripheral collisions.

In the proton-nucleus experiment reported here, no such restrictive trigger was applied. The reaction products of peripheral as well as central collisions were measured in a large solid angle and subjected to a  $(p, \pi)$  invariant mass analysis, in order to obtain the relevant information about the  $\Delta$ 's in the final state of the collision.

## 2. Experimental procedures

The systems under investigation were  $p + A$ , with protons at the two energies of 0.8 and 1.6 GeV, and  $A = \text{C, Nb}$  and  $\text{Pb}$  as targets. The experiment was performed at

$\star$  Dedicated to Prof. Dr. P. Kienle on the occasion of his 60th birthday

the SATURNE synchrotron (Saclay), using the large solid angle drift chamber of the DIOGENE-detector [7]. The experimental and data-reduction procedures have been described in [8]. Therefore, only a brief summary of those is presented here.

The cylindrical drift chamber covers the range of polar angle from  $14^\circ$  to  $143^\circ$  with full azimuthal symmetry. It is placed inside a magnetic field of 1 Tesla generated by a solenoid surrounding the chamber. Particle identification is achieved by means of the energy-loss momentum relation. As the DIOGENE-detector originally was designed for high multiplicity heavy-ion reactions ( $M \leq 40$ ) in a comparable energy range per nucleon, an excellent pion – proton separation up to 700 MeV/c is accomplished in the proton-nucleus collisions of this experiment, which has low multiplicity ( $M \leq 10$ ).

The detector resolution in momentum is  $\Delta p/p = 10$ –15% (FWHM), while the particle emission angles can be measured with an accuracy of  $2^\circ$ – $4^\circ$  (FWHM). The low energy cut-off for protons and pions due to energy-loss in the target and the beam-pipe are  $\sim 20$  MeV and  $\sim 10$  MeV respectively, depending on the emission angle.

The accumulated statistics of each system corresponds to roughly  $10^6$  events, with the exception of the carbon target at 1.6 GeV, where only half of this event number was measured.

Before being further analysed, each event has to pass software cuts in order to ensure well defined conditions. These software cuts are slightly more restrictive than those imposed by the detector onto the raw data.

First, a particle has to be emitted in an angular range of  $20^\circ \leq \Theta \leq 132^\circ$ . Then, low energy thresholds are defined in the  $p_t/m - y$  plane, where  $p_t/m$  denotes the transverse momentum normalized by the mass of the particle, and  $y$  is the rapidity. The same cuts as in [9] have been used, which are

for pions:

$$p_t/m \geq 0.60 + 1.29 y \quad (y < 0)$$

$$p_t/m \geq 0.60 - 0.96 y \quad (y \geq 0)$$

for protons:

$$p_t/m \geq 0.24 + 0.47 y \quad (y < -0.032)$$

$$p_t/m \geq 0.286 \quad (-0.032 \leq y < 0)$$

$$p_t/m \geq 0.24 - 0.62 y \quad (y \geq 0)$$

### 3. Experimental results

Within the detector's acceptance, the final state of a proton-nucleus reaction consists mainly of protons and of charged pions  $\pi^\pm$ . Composite particles ( $d, t, \alpha, \dots$ ) are also observed but they are not included in the analysis.

The minimum bias trigger defined by the software cuts above results in a total reaction cross-section of  $186 \pm 4(176 \pm 4)$ ,  $890 \pm 18(1009 \pm 20)$  and  $1258 \pm 50(1618 \pm 65)$  mb for C, Nb and Pb target at 0.8 GeV (1.6 GeV) incident proton energy. The resulting particle multiplicities of protons and pions for the carbon target

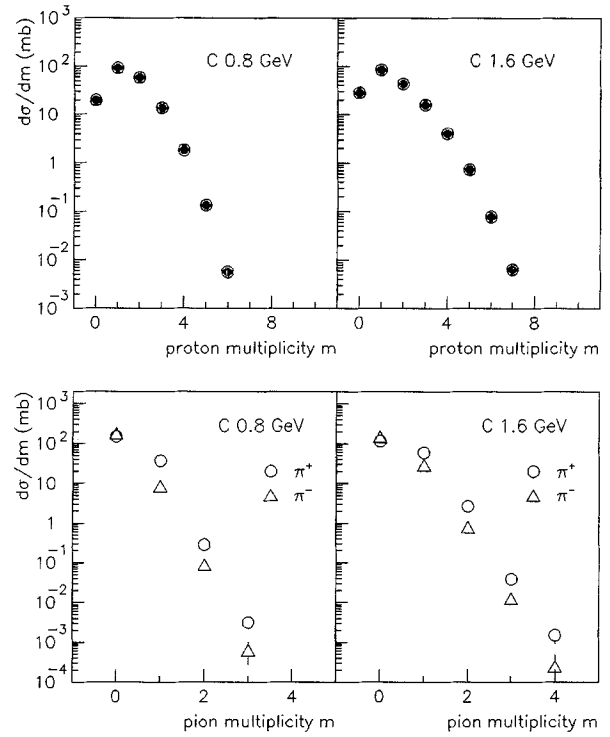


**Fig. 1.** Measured proton and pion multiplicities for the carbon target at 0.8 and 1.6 GeV incident proton energy

**Table 1.** Mean particle multiplicities for all targets at 0.8 GeV and 1.6 GeV incident proton energy. The statistical errors are less than  $\pm 1\%$

Target	$T_{\text{Lab}}(\text{GeV})$	$\langle m_p \rangle$	$\langle m_{\pi^+} \rangle$	$\langle m_{\pi^-} \rangle$
C	0.8	1.386	0.199	0.0465
Nb	0.8	1.614	0.119	0.0484
Nb	0.8	1.579	0.089	0.0469
C	1.6	1.354	0.363	0.171
Nb	1.6	2.025	0.254	0.170
Pb	1.6	2.069	0.202	0.163

at 0.8 and 1.6 GeV incident energy are shown in Fig. 1. These are rapidly decreasing distributions with mean multiplicities given in Table 1 for all systems.

A correlation analysis between protons and pions in the final state of a proton-nucleus reaction requires the selection of  $(p, \pi)$ -pairs after certain criteria. In the present experiment event-classes are defined according to the measured number of protons and pions per event. The analysis shows that only those classes with proton-multiplicities  $m_p = 1, 2, 3$  and a pion-multiplicity  $m_\pi = 1$  allow to identify the  $\Delta$  excitation unambiguously. It should be noticed that this type of event classification guaranties the same combinatorial background for each class. In addition, the classes with different multiplicities also belong to a slightly different range of impact parameter, as has been shown in [8]. Thus the chosen definition of different event-classes rests on a solid combinatorial as well as a physical foundation. The measured cross-sections for different event-classes are given in Table 2.

**Table 2.** The measured cross-section [mb] for the different event-classes within the detector-acceptance. The statistical error is less than  $\pm 1\%$

Target	$T_{\text{Lab}}$ (GeV)	$(m_p, \pi^+)$			$(m_p, \pi^-)$		
		$m_p=1$	2	3	$m_p=1$	2	3
C	0.8	14.62	3.47	0.374	3.19	2.36	0.88
Nb	0.8	41.55	14.06	2.7	15.62	11.39	3.87
Pb	0.8	44.05	13.28	2.24	23.73	14.63	3.99
C	1.6	21.99	9.7	2.72	9.56	7.16	3.569
Nb	1.6	75.81	52.63	26.56	41.99	41.75	29.41
Pb	1.6	98.29	66.25	32.63	65.29	64.14	42.61

In the following, event-classes are denoted as  $(m_p, \pi^\pm)$ , which gives the number of protons measured in coincidence with a  $\pi^+$  or a  $\pi^-$ .

#### 4. Invariant mass analysis

The unique information about  $\Delta$ 's is hidden in correlations between the  $\Delta$ 's decay particles  $p$  and  $\pi^+$  or  $p$  and  $\pi^-$  in the final state. However, these correlations are contaminated with contributions from background processes giving rise to uncorrelated  $(p, \pi)$  combinations.

The proton-pion correlations are analyzed in terms of the pair's invariant mass,  $M_{p\pi}^2 = (p_p + p_\pi)^2$ , where  $p_p$  and  $p_\pi$  are the particles four momenta. The invariant mass distribution for the carbon target at 1.6 GeV choosing the event-class  $(m_p = 1, \pi^+)$  is shown in Fig. 2a. From this distribution, no clear distinction between correlated and background contributions can be made. A common way to determine the background contribution is given by the so-called 'eventmixing' procedure: Protons and pions are taken from different events, but from the identical event-class.

The resultant uncorrelated  $(p, \pi)$  invariant mass distribution is shown in Fig. 2b. To reduce statistical fluctuations, this mass distribution contains ten times more mixed events than the non-mixed spectrum. By definition, the former distribution shows the phase space, which is available to uncorrelated  $(p, \pi^\pm)$ -pairs. Final state correlations are destroyed artificially. Hence it is assumed that the shape but not the magnitude of the background component in Fig. 2a is sufficiently well represented by the mixed invariant mass distribution of Fig. 2b. The validity of this assumption has been verified with the help of intra-nuclear-cascade calculations (INC, Sect. 6), which gives a full microscopical treatment of a proton-nucleus reaction.

Any proton - pion correlations within the chosen event-classes can be made obvious by comparing the original  $(p, \pi)$  invariant mass distribution with the one generated through event-mixing. This is done by calculating the difference of two distributions, where both were normalized to equal numbers of counts. The resultant 'correlation-signal' is shown in Fig. 2c. A clear structure shows up in the region of the  $\Delta(1232)$  reso-

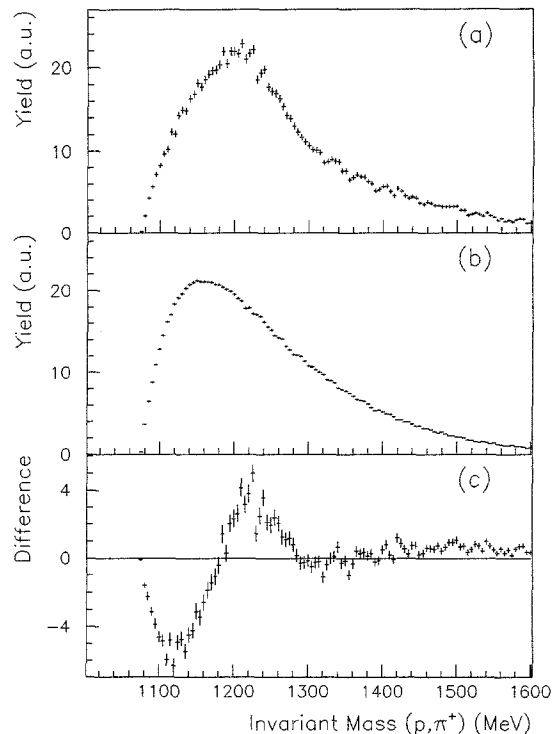


**Fig. 2.** **a** The  $(p, \pi^+)$  invariant mass distribution for the carbon target at 1.6 GeV proton energy and the event-class with  $m_p=1$ . **b** The corresponding mixed distribution, where proton and pion belong to different events but to the same event-class. **c** The difference of distribution a and b shows a clear 'correlation-signal' in the massregion of the  $\Delta$ -resonance

nance. As confirmation, the correlation-signal is also reproduced by INC calculations, and this proves the resonant origin of certain protons and pions in the final state.

These correlation-signals can be clearly seen in  $(p, \pi^+)$  as well as in  $(p, \pi^-)$  pairs for all systems with event-classes of proton-multiplicity  $m_p = 1, 2, 3$ .

As might be expected, the correlation-signal gets weaker with increasing proton-multiplicity because of the increase in combinatorial background, and weakens also with increasing target mass, since more and more wrong  $(p, \pi)$ -pairs are formed. Higher than  $m_p = 3$  classes show essentially only statistical fluctuations, which indicates the limit of resolving any contribution from  $\Delta$ -decay.

#### 5. The $\Delta$ -resonance

After verifying the presence of significant two-particle correlations between protons and pions within all event-classes due to the  $\Delta$ -decay, the next step is to extract the  $\Delta$  mass distribution, i.e. to determine the correlated part of the  $(p, \pi)$  invariant mass spectrum, and to find the mass  $E_0$  and width  $\Gamma$  of the  $\Delta$ -resonance.

The measured  $(p, \pi)$  invariant mass distribution, Fig. 2a, is composed of a correlated part, which should follow the shape of a modified Breit-Wigner distribution, and a non-correlated part, the shape of which is given

by event-mixing. An appropriate parametrization of the resonant  $\pi p$  cross-section is given by Cugnon [10]:

$$\sigma(\sqrt{s}) \sim \frac{q^3}{q^3 + \mu^3} \frac{1}{4 \left( \frac{\sqrt{s} - E_0}{\Gamma} \right)^2 + 1} \quad (*)$$

with  $\mu = 180 \text{ MeV}/c$ , while  $q$  is the momentum in the  $\pi p$  center of mass frame and  $\sqrt{s}$  is the total CM energy.  $E_0$  and  $\Gamma$  denote mass and decay-width of the resonance, which can be different in the nuclear medium from the free values  $E_0 = 1215 \text{ MeV}$  and  $\Gamma = 110 \text{ MeV}$  and which are treated as parameters to be determined by the fitting procedure. A third parameter  $\lambda$  has to be introduced which determines the size of the background component relative to the total  $(p, \pi)$  invariant mass spectrum.

Optimal values for  $E_0$ ,  $\Gamma$  and  $\lambda$  are obtained by means of a  $\chi^2$  minimization procedure which fits the expected invariant mass distribution to the measured one. As an example Fig. 3 shows the decomposition of the latter distribution into resonance and background contributions for all systems and for the event-class ( $m_p = 1, \pi^+$ ).

The results of the deduced mass  $E_0$  and width  $\Gamma$  for different event-classes for the optimal values of normalization parameter  $\lambda$  are given in Figs. 4, 5. It can be seen that an increasing proton-multiplicity leads to rising values of the  $\lambda$  parameter. The values  $E_0$ ,  $\Gamma$  of the free  $\Delta$ , within the used parametrization, are indicated by the dashed line.

One observes a significant reduction of the effective mass  $E_0$  with respect to the free value for almost all systems. In addition, the carbon data at 0.8 GeV suggest

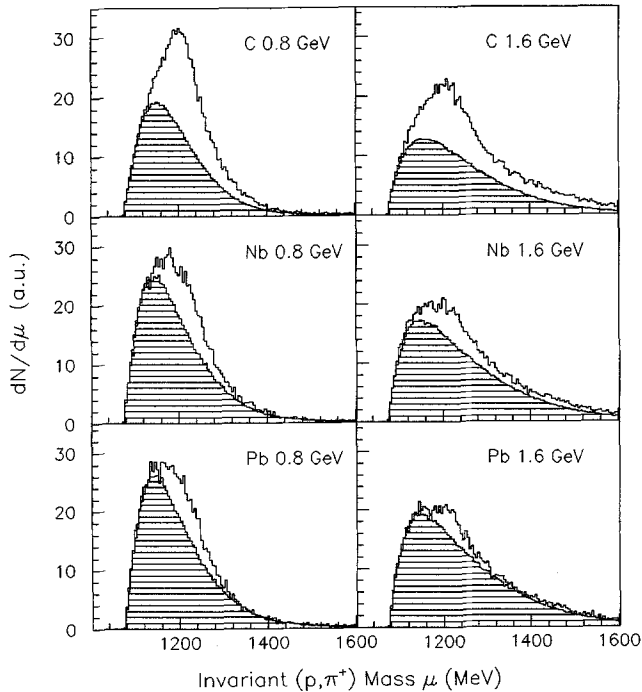


**Fig. 3.** The decomposition of  $(p, \pi^+)$  invariant mass distributions into a background (shaded) and a resonance part for all systems and those event-classes with  $m_p = 1$

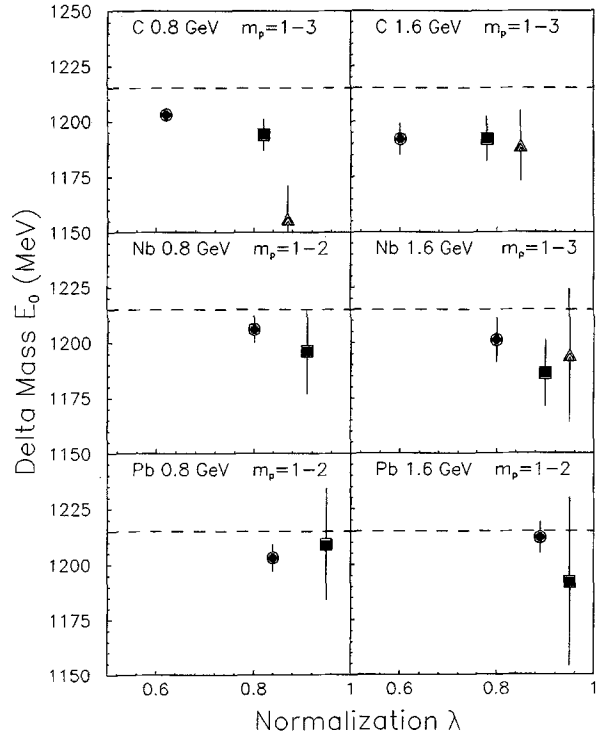


**Fig. 4.** Results for the effective  $\Delta$ -mass  $E_0$  for all systems and event-classes. The dashed line shows the free value within the used parametrization. Circles, squares and triangles correspond to event-classes of proton-multiplicity  $m_p = 1, 2$  and  $3$ , respectively

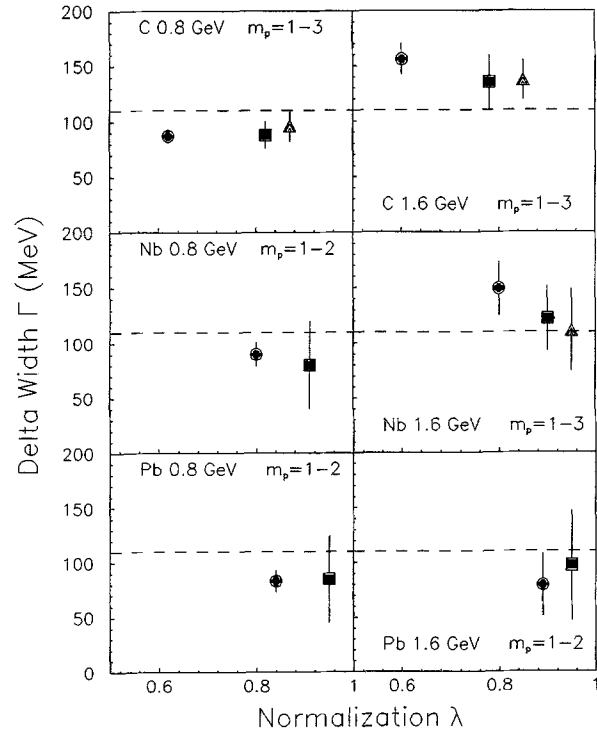


**Fig. 5.** Results for the effective  $\Delta$ -width  $\Gamma$ . The dashed line at  $110 \text{ MeV}$  indicates the free value within the used parametrization. Circles, squares and triangles correspond to event-classes of proton-multiplicity  $m_p = 1, 2$  and  $3$ , respectively

that this reduction increases with increasing multiplicity. The magnitude of this effect ranges from about  $-10$  MeV for  $m_p=1$  to almost  $-60$  MeV for the  $m_p=3$  event-classes.

The extracted values of  $\Gamma$  are, within the experimental uncertainties independent of the proton-multiplicity, but occur to be always smaller than the free value for the low beam energy and larger than the free value only for the high beam energy and the smallest system  $p+C$ . These findings, i.e. the dependence of  $E_0$  and  $\Gamma$  on beam energy and proton-multiplicity, indicate that the observed deviations from the free values are, at least partly, coupled to the energy depositions in the proton-nucleus collision. To investigate this coupling in more detail the collision dynamics was studied with the help of the intra-nuclear-cascade model (INC) of Cugnon [11], with its latest modification described in [10].

## 6. Comparison with INC

In simple terms, the INC-model treats a proton-nucleus collision as a succession of binary collisions, using the free cross-sections of elastic and inelastic NN and  $\pi N$  scattering. Inelasticity is taken into account via  $NN \rightarrow N\Delta$ , where the  $\Delta$  is treated as the free resonance. The subsequent decay of  $\Delta \rightarrow N\pi$  leads to the production of pions. Pion reabsorption has to proceed via the inverse reaction. Within the calculation, the whole history of a  $pA$  collision is recorded. This allows to label correlated  $(p, \pi)$ -pairs and to determine the background contributions directly. Thus it is possible to check the reliance

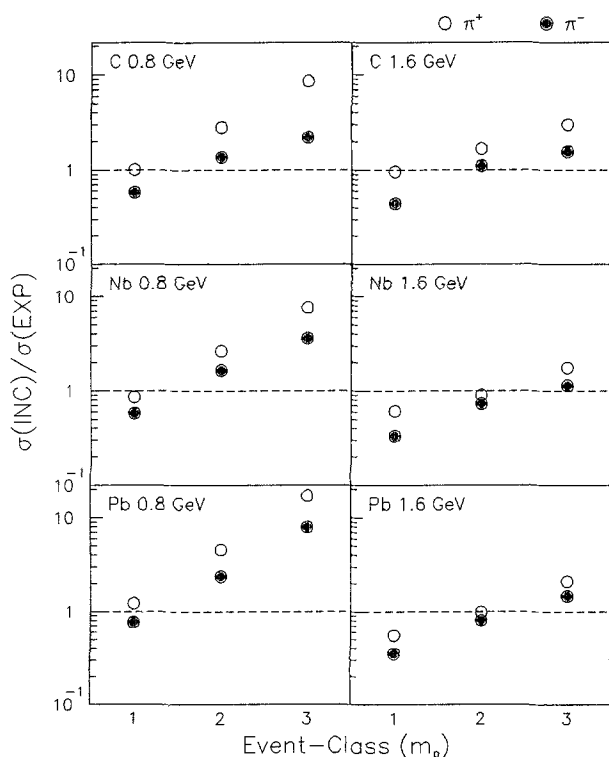


Fig. 6. The ratio of INC to experimental cross-sections for the different event-classes within the detector-acceptance

Table 3. The mean reduced impact parameter  $\langle b_r \rangle$  for all event-classes. The statistical error is less than  $\pm 0.06$

Target	$T_{\text{Lab}}$ (GeV)	$\pi^+$			$\pi^-$		
		$m_p=1$	2	3	$m_p=1$	2	3
C	0.8	0.65	0.56	0.49	0.62	0.59	0.50
Nb	0.8	0.72	0.62	0.57	0.70	0.63	0.56
Pb	0.8	0.76	0.67	0.61	0.76	0.66	0.60
C	1.6	0.67	0.57	0.50	0.66	0.60	0.52
Nb	1.6	0.79	0.68	0.61	0.76	0.70	0.62
Pb	1.6	0.83	0.74	0.66	0.82	0.74	0.68

of the analysis and to relate the experimental results to the properties of the fundamental two-particle collisions.

The INC data are subjected to the same software-cuts as the experimental data, and they are divided into the corresponding event-classes. Figure 6 gives for each class the ratio of the calculated cross-sections to the measured ones. At 0.8 GeV proton-energy, the  $(m_p=1, \pi^+)$  event-class is well reproduced by the model, while the  $(m_p=1, \pi^-)$  events are underestimated by  $\sim 40\%$ . All event-classes of higher multiplicity are overestimated by the cascade-model. At 1.6 GeV proton-energy, the best agreement is obtained for  $(m_p=2, \pi^\pm)$  event-classes, while  $m_p=1$  events are underestimated and  $m_p=3$  are clearly overestimated. Thus one general behaviour of the cascade-model dealing with nucleus-nucleus collisions, namely the production of too many pions, again appears in proton-nucleus reactions.

The comparison with the INC calculations also yields the mean impact parameters for the different event-classes. They are listed in Table 3 in terms of the reduced impact parameter  $b_r = b/b_{\text{max}}$ . As was already pointed out in [8], the discrimination on proton-multiplicity introduces an impact parameter variation, with a large variance of the  $b_r$ -distribution for a given  $m_p$ . As composite particles play only a minor role in these  $pA$  collisions, the error in the relation between  $\langle b_r \rangle$  and  $m_p$ , made by neglecting ‘pseudo-protons’ [8], is believed to be small. Very peripheral  $pA$  collisions, which produce quasi-free  $\Delta$ -excitation processes like in ref. [12], are excluded in the present experiment by the limited detector acceptance for the very forward angles.

The INC calculations allow the conclusion, that the  $\Delta$ 's are produced inside nuclear matter in the very first NN collisions. But the pions, emitted in the decay of primary  $\Delta$ 's, are mostly reabsorbed and form new baryon resonances, whereas the correlated nucleons are likely to scatter again. Thus the information on primary  $\Delta$ 's is nearly completely destroyed.

Within the INC-model, it is possible to follow the development of several  $\Delta$  ‘generations’, characterized by the collision-number in which they were excited. Figure 7 shows for the carbon and lead targets the  $\Delta$  mass distribution of the first generation, i.e.  $\Delta$ 's generated in the very first NN-collision, in comparison with the last generation. The protons and pions from the decay of this

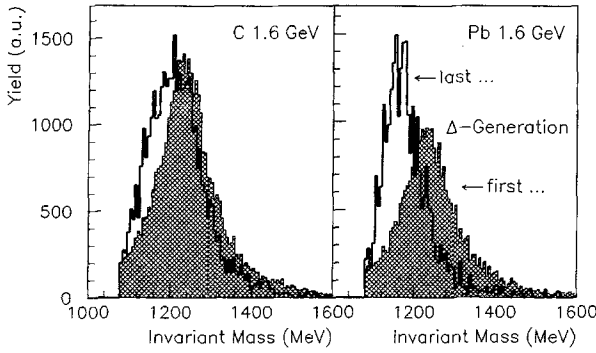


**Fig. 7.** Comparison of the  $\Delta$  mass distributions of the first and the last  $\Delta$ -generation inside the cascade-calculation for carbon and lead target at 1.6 GeV

$\Delta$  generation are those, that are finally detected. The results of Fig. 7 include all event-classes. While the resonance shape of the first  $\Delta$ 's are very close to the free one, the mean energy of the last generation is clearly shifted towards lower masses. The cascade-model treats the  $\Delta$  excitation via  $NN \rightarrow N\Delta$  and  $\pi N \rightarrow \Delta$  in terms of free cross-sections. Thus the observed shift can only be interpreted as a consequence of multiple scattering or reabsorption of nucleons and pions. Since the number of binary collisions increases with target mass, the shift for lead is larger than for the light carbon target. Within the frame of the cascade-model, a direct relation between the number of multiple collisions and mass-shift is predicted. Furthermore the collision-number is also related to the proton-multiplicity. A decrease of the  $\Delta$  mass with increasing multiplicity is therefore predicted and clearly observed in the experimental carbon data at 0.8 GeV. The magnitude of the predicted shift is of the same order as observed.

It must be concluded, that in addition to possible in-medium modifications of the  $\Delta$ , a shift of its effective mass  $E_0$  in the order  $-10$  MeV to  $-60$  MeV results from the rather trivial multi-scattering of nucleons and reabsorption of pions. The comparison to the INC results does not allow these in-medium effects on the  $\Delta$  mass to be larger than  $\pm 10$  MeV for those  $\Delta$ 's that were identified in the present experiment.

The cascade-calculations include only the excitation of the  $\Delta$  degree of freedom and neglect heavier baryon states. A direct comparison of calculated and experimental  $(p, \pi^+)$  and  $(p, \pi^-)$  mass-distributions, which have been properly corrected for the background and therefore represent pure resonance mass-distributions, reveals to which extent the  $\Delta$ 's dominance can be justified. Figure 8 gives this comparison for the light carbon target at 1.6 GeV and for the event-classes with  $m_p=1$ . For correlated  $(p, \pi^+)$ -pairs measured, a shoulder at about 1500 MeV shows up which is clearly not contained in the INC-data. The difference between INC and experiment is even more pronounced in the case of  $(p, \pi^-)$ . In contrast to the calculation, the experiment yields a broad mass-distribution, very distinct from a pure  $\Delta$  resonance shape. It is concluded, that the population of  $N^*$ -states occurs in this mass-region. Since no trigger on peripheral, quasi-elastic excitation was used, no sec-

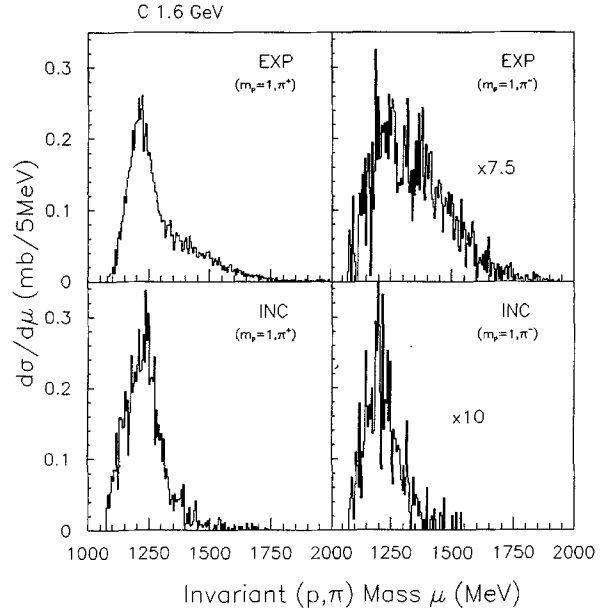


**Fig. 8.** Comparison of the line-shapes of the  $\Delta^{++}$  and  $\Delta^0$  mass distributions in INC and experiment for the carbon target at 1.6 MeV and the  $(m_p=1, \pi^\pm)$  event-classes. As the cascade-model contains only the  $\Delta$  degree of freedom, there is clear evidence for the excitation of higher baryon states than  $\Delta(1232)$ , in  $(p, \pi^+)$  and even more pronounced in  $(p, \pi^-)$  pairs

**Table 4.** The cross-section of total  $\pi^\pm$ -production for all systems and the fraction of the emission of correlated  $(p, \pi)$  pairs

Target	$T_{\text{Lab}}$ (GeV)	$\pi_{\text{tot}}^+$ [mb]	$\pi_{\text{corr}}^+/\pi_{\text{tot}}^+$	$\pi_{\text{tot}}^-$ [mb]	$\pi_{\text{corr}}^-/\pi_{\text{tot}}^-$
C	0.8	$45.6 \pm 1$	$0.27 \pm 0.03$	$10.6 \pm 0.4$	$0.36 \pm 0.06$
Nb	0.8	$127.0 \pm 5$	$0.16 \pm 0.03$	$48.9 \pm 2.6$	$0.20 \pm 0.07$
Pb	0.8	$131.4 \pm 6$	$0.11 \pm 0.03$	$63.0 \pm 3.6$	$0.10 \pm 0.04$
C	1.6	$79.7 \pm 2$	$0.35 \pm 0.03$	$37.4 \pm 1$	$0.36 \pm 0.08$
Nb	1.6	$308 \pm 11$	$0.29 \pm 0.06$	$206 \pm 7$	$0.10 \pm 0.03$
Pb	1.6	$399 \pm 18$	$0.14 \pm 0.05$	$296 \pm 14$	$0.17 \pm 0.1$

ond resonance peak shows up like in [12], but multi-scattering processes lead to a broadening of the distribution. Above 1.5 GeV, the necessity of including  $N^*$  resonances to describe NN inelastic scattering was already pointed out in [13, 14].

Another information that can be accessed by the present experiment are the cross-sections for correlated  $(p, \pi)$  emission. The measured cross-section for this process is taken as the sum over all relevant event-classes. In addition, certain correction factors have to be applied to account for the limited detector acceptance. These numbers are taken from the cascade-calculations, and the final cross-sections are expressed as the ratio to the inclusive total  $\pi^\pm$  cross-sections. The results are given in Table 4.

## 7. Discussion and conclusion

While the measured  $(p, \pi)$  invariant mass distribution and its mixed counterpart are well defined within a cho-

sen event-class, the extraction of the pure  $\Delta$  mass distribution relies on the assumption that it follows a Breit-Wigner form. The approximate validity of this assumption not only decides upon the background normalization  $\lambda$  but it also influences the values of the extracted resonance parameters  $E_0$  and  $\Gamma$ .

An independent estimate of  $\lambda$  can be obtained by the following considerations. An upper limit of  $\lambda$  is given by the requirement, that the  $\Delta$  mass should be positive from the threshold energy to the maximum available energy. If  $\lambda$  is chosen too large, the subtraction of the background results in non-physical, negative values of the mass distribution at threshold, similar to the correlation-signal. It turns out, that the  $\chi^2$ -fit procedure gives values of  $\lambda$ , which are very close to this upper-limit value, where a correct treatment of the threshold behaviour of the  $\pi p$  scattering cross-section is essential. Differences for the  $\lambda$  parameter appear on a scale less than  $\pm 0.025$ .

Another source of independent information on  $\lambda$  are the INC calculations. The cascade results agree with the extracted experimental values within  $\pm 0.05$ . Thus it is concluded, that the numbers for  $\lambda$  given in Figs. 4, 5 are correct within a combined error of  $\pm 0.06$  and independent of the correct shape of the  $\Delta$  resonance.

The resonance mass  $E_0$  and its width  $\Gamma$  were obtained by fitting the modified Breit-Wigner mass distribution. In view of the INC results the use of (\*) does not need to be correct a priori. But the goodness of the  $\chi^2$  fits indicates that (\*) still describes the invariant mass distribution although it is the result of several  $\Delta$  generations and modified by the collision dynamics.

Alternatively,  $E_0$  may be defined as the mean energy of the invariant mass distribution and compared to the corresponding quantity from the INC calculations. The results were found to be very similar to the ones already presented: One observes an experimental reduction of  $E_0$  which is close to the reduction expected from the collision dynamics and therefore leaves very little room for any in-medium effects.

In order to substantiate this conclusion, a more reliable transport-model is needed, which includes both, a density dependent medium-modification of the  $\Delta$  and a correct treatment of the  $\Delta$  propagation out of the reaction-zone to the surface, where the decay particles finally can be measured experimentally.

In conclusion, the cascade-model reveals the importance of simple phase-space considerations for the  $\Delta$  mass distribution in the final state of a  $pA$  collision. Discrepancies between INC and experiment, which may indicate the influence of the medium, are of the order of  $\pm 10$  MeV. The main systematic uncertainty in this number comes from the background subtraction and from possible, small distortions of the modified Breit-Wigner line-shape.

The smallness of the in-medium effects deduced here, is not totally unexpected, since the observed  $\Delta$  are mostly from a late generation, when the expanding nuclear matter has already low density.

## References

- Cugnon, J., Mizutani, T., Vandermeulen, J.: Nucl. Phys. A **352**, 505 (1981);  
Stock, R., Bock, R., Brockmann, R., Harris, J.W., Sandoval, A., Ströbele, H., Wolf, K.L., Pugh, H.G., Schroeder, L.S., Maier, M., Renfordt, R.E., Dacal, A., Ortiz, M.E.: Phys. Rev. Lett. **49**, 1236 (1982);  
Cahay, M., Cugnon, J., Vandermeulen, J.: Nucl. Phys. A **411**, 524 (1983);  
Harris, J.W., Odyniec, G., Pugh, H.G., Schroeder, L.S., Tincknell, M.L., Rauch, W., Stock, R., Bock, R., Brockmann, R., Sandoval, A., Ströbele, H., Renfordt, R.E., Schall, D., Bangert, D., Sullivan, J.P., Wolf, K.L., Dacal, A., Guerra, C., Ortiz, M.E.: Phys. Rev. Lett. **58**, 463 (1987)
- Molitoris, J.J., Stöcker, H., Winer, B.L.: Phys. Rev. C **36**, 220 (1987)
- Aichelin, J., Rosenhauer, A., Peilert, G., Stöcker, H., Greiner, W.: Phys. Rev. Lett. **58**, 463 (1987); Gale C.: Phys. Rev. C **36**, 2152 (1987)
- Schönhofen, M., Cubero, M., Gering, M., Sambataro, M., Feldmeier, H., Nörenberg, W.: Nucl. Phys. A **504**, 875 (1989)
- L'Hôte, D. et al.: Corinne 90, 387 Nantes, June (1990)
- Ellegaard, C. et al.: Phys. Rev. Lett. **50**, 1745 (1983);  
Contardo, D. et al.: Phys. Lett. **168B**, 331 (1986); Gaarde C.: Nucl. Phys. A **478**, 475 (1988)
- Delorme, J., Guichon, P.A.M.: 10<sup>e</sup> Session d'études biennale de Physiques Nucléaire Aussois (1989), LYCEN Report 8902
- Alard, J.P., Arnold, J., Augerat, J., Babinet, R., Bastid, N., Brochard, F., Costilhes, J.P., Crouau, M., deMarco, N., Drouet, M., Dupieux, P., Fanet, H., Fodor, Z., Fraysse, L., Girard, J., Gorodetzky, P., Gosset, J., Laspalles, C., Lemaire, M.-C., L'Hôte, D., Lucas, B., Montarou, G., Papineau, A., Parizet, M.J., Poitou, J., Racca, C., Schimmerling, W., Tamain, J.C., Terrien, Y., Valero, J., Valette, O.: NIM A **261**, 379 (1987)
- Lemaire, M.-C., Trzaska, M., Alard, J.P., Augerat, J., Bachelier, D., Bastid, N., Boyard, J.-L., Cavata, C., Charmensat, P., Cugnon, J., Dupieux, P., Gorodetzky, P., Gosset, J., Hennino, T., Jourdain, J.-C., LeMerdy, A., L'Hôte, D., Lucas, B., Marroncle, J., Montarou, G., Parizet, M.J., Poitou, J., Quassoud, D., Radvanyi, P., Ramstein, B., Rahmani, A., Roy-Stephan, M., Valette, O., Vandermeulen, J., Zupranski, P.: LNS-preprint (LNS/Ph/90-30), (accepted by Phys. Rev. C)
- Cavata, C.: Thèse, Université de Paris XI, Orsay 1989
- Cavata, J., Lemaire, M.-C.: Nucl. Phys. A **489**, 781 (1988)
- Cugnon, J., Kinet, D., Vandermeulen, J.: Nucl. Phys. A **379**, 553 (1982);  
Cugnon, J., Lejeune, A., Grangé, P.: Phys. Rev. C **35**, 861 (1987);  
Cugnon, J.: Nucl. Phys. A **402**, 751 (1987)
- En'yo, H.: Thesis, University of Tokyo 1985;  
Nagae, T. et al.: Phys. Lett. **191B**, 31 (1987);  
Chiba, J., Nucl. Phys. A **478**, 491 (1988)
- Lock, W.O., Measday, D.F.: 'Intermediate energy nuclear physics'. London: Methuen & Co. Ltd. 1970
- VerWest, B.J., Arndt, R.A.: Phys. Rev. C **25**, 1979 (1982)